AUTOMATIC PREDICTION OF BREAST CANCER METASTASIS STAGES VIA DEEP CONVOLUTIONAL NETWORKS

Shenghua Cheng, Shaoqun Zeng, Jiangsheng Yu

Huazhong University of Science and Technology, Bingsheng Technology Company, Wuhan, China

ABSTRACT

Automatic and accurate detection of breast cancer metastases is meaningful for reducing the workload of the pathologists and reducing the cost of diagnosis. In this paper, we presented a learning-based method for automated prediction of breast cancer metastasis stages. This method is trained and validated on Camelyon17 challenge datasets. The method consists of three parts: tissue extraction, tumor region detection and cancer metastasis stage prediction.

Index Terms – Cancer metastases prediction, deep convolutional networks, Camelyon17 challenge

1. INTRODUCTION

Breast cancers metastasis diagnosis needs the analysis of hematoxylin and eosin stained slides [1]. Currently, the slides are examined done by pathologists manually. But this manual examination depends on the experience of the pathologists and is subjective and time-consuming. The centimeter-scale sections are imaged at sub-micrometer resolution, thus, the resulting whole slide images (WSIs) are of Gigapixels. Manual check of the WSIs is very tedious and easily misses small regions. Therefore, automatic and accurate detection of breast cancer metastases is meaningful for reducing the workload of the pathologists and reducing the cost of diagnosis. Recent Camelyon16 and 17 challenges promote the development of cancer automatic detection algorithms in pathology WSIs [2-4]. The key of these methods is how to predict tumor regions in WSIs at pixel level. Compared traditional model-based or hand-crafted features methods, deep learning is data-driven methods and can learn hierarchical feature representation automatically [5]. In image classification and semantic segmentation fields, deep convolutional networks have archived great successes in recent years [6-7]. Therefore, we adopt deep convolutional networks to predict tumor region in WSIs at pixel level.

The goal of Camelyon17 [8] is to predict the pN-stage of each patient, which is decided by the metastasis status of his five lymph node WSIs. Thus, the key is to accurately predict WSI metastasis status (normal, isolated tumor cells, micro-metastases and macro-metastases). To solve this problem, this paper presented a method consisting of three parts: tissue extraction, tumor region detection and patient pN-stage prediction. The tissue region extraction is based on the difference of pixel RGB values. The tumor regions in WSIs are detected by GoogLeNet-v3 finetuned on the ImageNet weights [7]. The WSI status is classified by random forest algorithm with morphological features extracted from the predicted tumor heatmap, then the pN-stage can be obtained by the given rule. There are three key points for accurately predicting cancer metastasis stages: 1) effectively deal with the imbalance of tumor and normal samples and the imbalance of tumor regions of various cases (isolated tumor cells, micro-metastases and macro-metastases); 2) how to train the very deep network on the limited datasets of simple samples and hard samples; 3) how to prevent overfitting when learning a classifier of WSI metastasis status on 500 WSIs. Aiming at these challenges, we designed some effective strategies for training sample preparation (Section 2.3.1), network training (Section 2.3.2) and the WSIs metastasis status classification (Section 2.4). This method is inspired by the method in [3].

2. METHODS

The presented method includes three parts: tissue extraction (Section 2.2), tumor region detection (Section 2.3.1) and cancer metastasis stage prediction (Section 2.3.2). Diagram of the method is depicted in **Fig. 2**.

2.1. Datasets

The training and testing datasets come from Camelyon16 [9] and 17 challenges [8] . The finished Camelyon16 challenge contains 160 tumor WSIs with tumor region labelling and 240 normal WSIs. The Camelyon17 challenge contains 100 patients (5 WSIs per patient) with pN-stage classification. 50 WSIs of the 500 WSIs have tumor region annotation. Another 100 patients are provided for testing. In tumor region detection stage, we used all the WSIs with annotation and normal WSIs as our training datasets.

2.2. Extraction of Tissue Region

The whole slide pathological images (WSIs) usually contain a lot of non-tissue blank regions. Thus, we design a method to extract the tissue regions from the WSIs . Post tumor region detection is then constrained on the extracted tissue regions. After observation, we found that the tissue and non-tissue regions can be classified by the pixel color. The colored region are more possibly be the tissue region. Therefore, we use the different of the maximum and minimum values of pixel RGB values to evaluate the colored degree. Tissue foreground masks can be obtained with a threshold 10. Holes on the masks are filled with morphological operations. We found this method is simpler than the common OTSU method [10] but is valid for tissue region extraction in WSIs (**Fig. 1**)

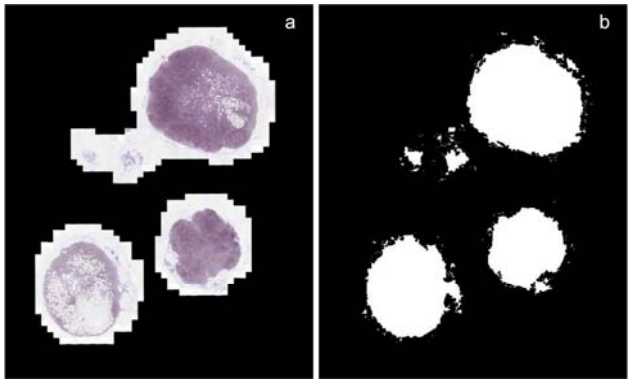

Fig. 1. RGB-based tissue region extraction. **a** is the original WSI of patient 0 node 2. **b** is the extracted tissue mask. If the different of the maximum and minimum values of a pixel RGB values is greater than 10, the pixel is labeled as tissue region. Holes on the masks are filled with morphological operations. All tissue regions in the WSI have been labelled in its entirety the method.

2.3. Learning-based Tumor Region Detection

We adopt patch-based GoogLeNet-v3 classification network for distinguishing tumor regions from normal regions.

2.3.1. Preparation of training samples

From each tumor WSIs with annotation, we randomly (with uniform distribution) select 2K positive patches in tumor regions and 20K negative patches in normal regions. From each normal WSIs, we randomly select 20K negative patches. For each training epoch, we randomly sampling the same number of positive/negative patches. The strategy has several advantages: 1) positive patches are sampled from each tumor WSIs with the same probability, thus, WSIs with small tumor regions will be not be ignored in the training; 2) the imbalance of positive and negative patches is dealt with by resampling. The patch size is set to 299×299, which can contain enough cells in a patch as recognition context. The RGB values of a patch are normalized into [-1 1]. No sample augmentation has been done. In addition, 2K positive patches and 2K negative patches are extracted from the tumor-normal boundary region of each tumor WSI. These hard samples are prepared for improving the detection accuracy of the network. The network training consists of multiple rounds from simple samples to hard samples.

2.3.2. Network training

We adjust the last fully connected layer of GoogLeNet-v3 to 2 classes. We finetune the network with the ImageNet weight. Specifically, we freeze the bottom 287 layers of GoogLeNet-v3 and train the top layers on simple samples with 0.01 learning rate. Then, we only freeze the bottom 200 layers and train the others on simple samples and boundary hard samples with 0.001 learning rate. We use the resulted network to test all training datasets, and generate the false positive and the false negative samples. Finally, we finetune the top layers (except the bottom 200 layers) on the simple samples, boundary hard samples and these misclassified samples with 0.001 learning rate. The step-by-step finetuning strategy has the following advantages: 1) we take full use of the ImageNet weights trained on a huge number of images with various categories, the shallow-layer feature representations of which are very robust and common; 2) the network is

easier to converge from the simple samples to hard samples. The network is trained with Adam method [11].

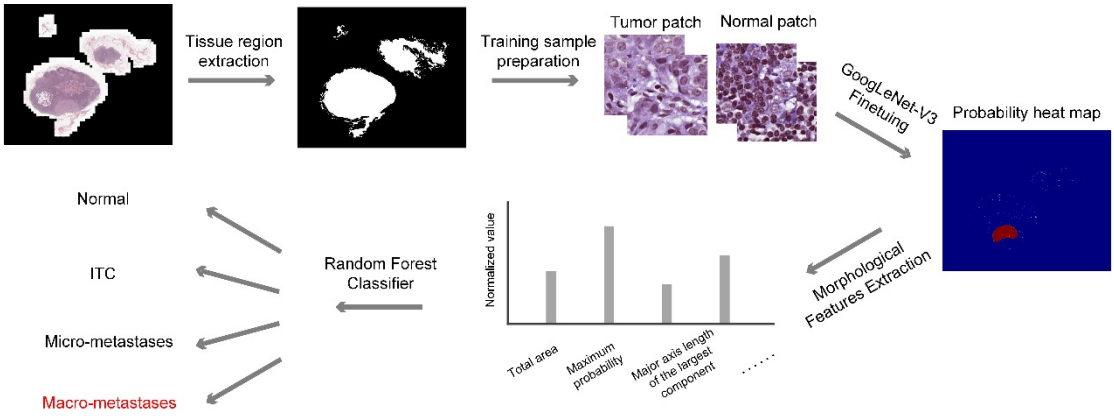

Fig. 2. The diagram of the presented learning-based method of cancer pN-stage prediction.

2.4. Prediction of Patient pN-stage

For each WSI, we divide it into a number of patches with a stride *s*. Then, we can obtain a tumor region prediction heatmap of each WSI with a resolution *s* using the trained network. Some morphological operations are used to fill the holes and close the small gaps of the binarized heatmap. 13 morphological features (**Table 1**) of a binarized WSI heatmap are extracted for classification the WSI into four states: normal, ITC (isolated tumor cells), micro-metastases and macro-metastases. Since we only have 500 WSIs for training and validation, the key of this part is how to prevent overfitting with the small dataset. We use random forest algorithm to learn WSI state classification on the Camelyon17 datasets. K-fold cross validation is adopted for preventing overfitting and adjusting hyperparameters (WSI heatmap binarization threshold and random forest hyperparameters). The randomness of feature selection and subset selection when generating decision trees helps preventing overfitting. Finally, we can obtain the patient pN-stage using the given rule. **Fig. 2** shows the diagram of the presented method.

Table 1. The 13 morphological feature of a binarized WSI heat map.

Feature Number	Feature Name	Feature Number	Feature Name
1	Total area	8	Maximum probability of the largest component
2	Maximum probability	9	Minor axis length of the largest component
3	Average probability	10	Average probability of the largest component
4	Area of the largest component	11	Extent of the largest component
5	Convex area of the largest component	12	Solidity of the largest component
6	Major axis length of the largest component	13	Eccentricity of the largest component
7	Equivalent Diameter of the largest component		

3. EXPERIMENTS

We trained our tumor region detection network on Camelyon16 and 17 datasets (all manually labelled tumor WSIs and all normal WSIs). The training accuracy (patch classification accuracy) achieved 0.98 within several days.

The training was implemented in Keras [12] with Tensorflow [13] backend using one GTX 1080Ti. In application stage, we got the heatmaps with the stride 128 for reducing computing time. Generating one WSI heatmap needs about 10~20 minutes.

The random forest for classifying the WSI status was trained on Camelyon17 training dataset (500 WSIs). Because the small number of cases, 5-fold cross validation was utilized to search good hyperparameters. We obtained 0.86 average validation accuracy of WSIs status classification.

4. DISCUSSIONS

In the paper, we presented learning-based method for automatic prediction of breast cancer metastasis stage. This method consists of three parts: tissue extraction, tumor region detection with deep convolutional networks and cancer metastasis stage prediction with random forest. The method was demonstrated to be effective on Camelyon17 datasets.

The shortcoming of the method is its speed of generating heatmap for using patch-based classification network and scanning strategy. The speed, 10~20 minutes per WSI heat map using one GTX1080Ti, is very limited for thousands of WSIs. Furthermore, the resolution of heatmap is very low (depending on the stride *s*). Thus, we cannot predict tumor region boundary accurately, and the small tumor regions maybe missed using the low-resolution heatmap. Fully connected convolutional networks [14,15] are more suitable for dense prediction task or semantic segmentation. We experimented the fully connected convolutional network with atrous spatial pyramid pooling [15], and one WSI heatmap at level 0 can be obtained within 3~5 minutes. But the convergence of the fully connected convolutional network is more difficult. More detailed researches are underway.

5. REFERENCES

[1] Fischer, A. H. et al. Hematoxylin and eosin staining of tissue and cell sections. *Cold Spring Harbor Protocols* **2008**, pdb-prot4986 (2008).

[2] Litjens, G. et al. Deep learning as a tool for increased accuracy and efficiency of histopathological diagnosis. *Scientific Reports* **6**, 26286 (2016).

[3] Wang, D. et al. Deep learning for identifying metastatic breast cancer. *arXiv preprint arXiv*, 1606.05718 (2016).

[4] Liu, Y. et al. Detecting cancer metastases on gigapixel pathology images. *arXiv preprint arXiv*, 1703.02442 (2017).

[5] LeCun, Y., et al. Deep learning. *Nature* **521**, 436-444 (2015).

[6] Krizhevsky, A. et al. Imagenet classification with deep convolutional neural networks. *Advances in Neural Information Processing Systems*, 1097-1105 (2012).

[7] Szegedy, C. et al. Rethinking the inception architecture for computer vision. *Proceedings of the IEEE Conference on Computer Vision and Pattern Recognition*, 2818-2826 (2016).

[8] Geessink, O. et al. Camelyon17: Grand challenge on cancer metastasis detection and classification in lymph nodes, 2017.

[9] Bejnordi, B. E. et al. Camelyon16: Grand challenge on cancer metastasis detection in lymph nodes, 2016.

[10] Otsu, N. A threshold selection method from gray-level histograms. *IEEE transactions on systems, man, and cybernetics* **9**, 62–66 (1979).

[11] Kingma, D. et al. Adam: A method for stochastic optimization. *arXiv preprint arXiv*, 1412.6980 (2014).

[12] Chollet, F. Keras (2015). Available at: http://keras. io (2017).

[13] Bastien, F. et al. Theano: new features and speed improvements. *arXiv preprint arXiv*, 1211.5590 (2012).

[14] Long, J. et al. Fully convolutional networks for semantic segmentation. *In Proceedings of the IEEE Conference on Computer Vision and Pattern Recognition*, 3431-3440 (2015).

[15] Chen, L. C. et al. Deeplab: Semantic image segmentation with deep convolutional nets, atrous convolution, and fully connected crfs. *arXiv preprint arXiv*, 1606.00915 (2016).